

Key Points:

- Surface velocities in the Gulf of Maine Coastal Current have slowed on inter-decadal timescales, particularly southwest of Penobscot Bay
- An intensification of the southwesterly component of the winds in the region likely contributed to the observed changes

Correspondence to:

K. C. Burkholder,
kburkholder@stonehill.edu

Citation:

Burkholder, K. C., Lee, J. H., Kime, M., Calabro, C., & Manning, J. P. (2024). Decadal-scale variability in the surface flow of the Gulf of Maine Coastal Current: The impact of changing climate conditions on coastal circulation. *Journal of Geophysical Research: Oceans*, 129, e2023JC020512. <https://doi.org/10.1029/2023JC020512>

Received 22 SEP 2023

Accepted 24 MAR 2024

Author Contributions:

Conceptualization: Kristin C. Burkholder, James P. Manning
Formal analysis: Kristin C. Burkholder, Jane HyoJin Lee
Investigation: Kristin C. Burkholder, Jane HyoJin Lee, Meredith Kime, Cassandra Calabro
Methodology: Kristin C. Burkholder, Jane HyoJin Lee, James P. Manning
Validation: Kristin C. Burkholder, Jane HyoJin Lee
Visualization: Kristin C. Burkholder, Jane HyoJin Lee, Cassandra Calabro
Writing – original draft: Kristin C. Burkholder
Writing – review & editing: Kristin C. Burkholder, Jane HyoJin Lee, James P. Manning

Decadal-Scale Variability in the Surface Flow of the Gulf of Maine Coastal Current: The Impact of Changing Climate Conditions on Coastal Circulation

Kristin C. Burkholder¹ , Jane HyoJin Lee² , Meredith Kime^{1,3}, Cassandra Calabro¹, and James P. Manning⁴ 

¹Department of Environmental Sciences and Studies, Stonehill College, Easton, MA, USA, ²Department of Mathematics, Stonehill College, Easton, MA, USA, ³Department of Earth and Environmental Sciences, Columbia University, New York, NY, USA, ⁴National Oceanic Atmospheric Administration, Northeast Fisheries Science Center, Woods Hole, MA, USA

Abstract The Gulf of Maine (GOM) is one of the most productive and ecologically important marine environments on the planet. The Gulf of Maine Coastal Current (GMCC), which stretches along the western side of the GOM from the Bay of Fundy to Cape Cod, plays an important role in supporting this productivity by transporting nutrients, larvae and dinoflagellates southwestward along the Canadian and New England coastlines. Climate change has led to alterations in GOM ecosystems in recent years: GOM water temperatures have warmed and distributions of marine species have shifted. However, the impacts of the changing climate on the circulation within the GOM, including the path and velocity of the GMCC, have remained unclear. Here, we examine data collected by satellite tracked surface drifters and velocity data collected by the NERACOOS buoy array in order to investigate inter-decadal changes to the flow of the GMCC. We find that over inter-decadal timescales, the alongshore surface flow of the GMCC has slowed, particularly in the region southwest of Penobscot Bay. The slowdown observed in the GMCC surface flow is most likely attributed to a local strengthening of the southwesterly winds over the time period of interest.

Plain Language Summary The Gulf of Maine (GOM) is the region of the ocean stretching between the Bay of Fundy and Cape Cod. The GOM is well known as a productive fishery and an important habitat for endangered species. The biological productivity of the GOM relies on the transport of things like nutrients and larvae throughout the region. In the western GOM, much of this transport is carried out by the Gulf of Maine Coastal Current (GMCC), which stretches from the Bay of Fundy to Cape Cod. Unfortunately, climate change is impacting the GOM: record breaking temperatures and changes in the distribution of species have been observed in recent years. In this study, we use data collected from surface drifters and anchored buoys to investigate whether the waters of the GMCC are changing as the temperatures warm. The results of this study indicate that the surface flow of the GMCC has slowed, particularly in the region southwest of Penobscot Bay. This slowdown is likely due to an increase in the strength of the local winds from the southwest, which may have disrupted the southwestward flow of the surface waters.

1. Introduction

The Gulf of Maine (GOM), a semi-enclosed marginal sea stretching from Nova Scotia to Cape Cod, is one of the most complex and biologically diverse marine environments on the planet (Sherman & Skjoldal, 2002). The nutrient-rich waters of the GOM support high levels of primary productivity, which in turn support an ecosystem of both biological and economic importance. Surveys of biodiversity within the GOM have identified over 3,000 species of flora and fauna within its bounds (Valigra, 2006). The gross domestic product of the GOM economy has been estimated to be over \$500 billion (Thompson, 2010). Clearly, the GOM is a valuable resource worthy of study and protection.

Much of the amazing productivity of the GOM is reliant upon the effective circulation of inorganic nutrients throughout its waters. The circulation within the GOM is predominantly cyclonic (Bigelow, 1927; Brooks & Townsend, 1989) (Figure 1). Waters enter the region through the Northeast Channel (NEC) and are transported around the GOM by a series of interconnected currents. The work presented herein focuses on one section of this interconnected system: the Gulf of Maine Coastal Current (GMCC), which stretches along the western side of the GOM from the Bay of Fundy to Cape Cod. The GMCC is divided into two branches: the Eastern Maine

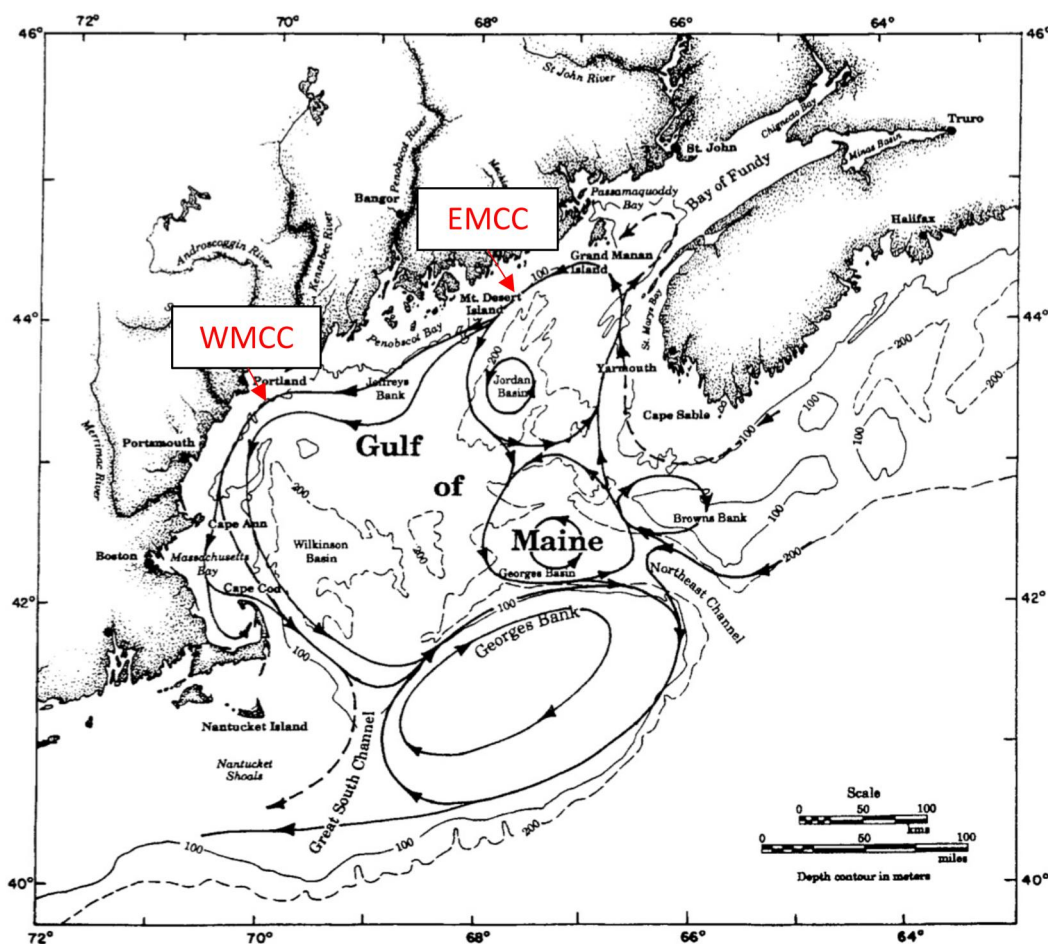


Figure 1. Circulation in the GOM is primarily cyclonic. The GMCC stretches along the western side of the GOM from the Bay of Fundy to Cape Cod and is divided into two branches: the Eastern Maine Coastal Current (EMCC) and the Western Maine Coastal Current (WMCC). Very slightly modified from Xue et al. (2000). © American Meteorological Society. Used with permission.

Coastal Current (EMCC) and the Western Maine Coastal Current (WMCC). The EMCC begins as GOM waters exit the Bay of Fundy and reliably extends down the coast as far as Penobscot Bay before partially veering offshore in the direction of George's Bank. The relative amount of water that veers offshore or continues down the coast as part of the WMCC varies substantially through time (Brooks & Townsend, 1989; Churchill et al., 2005; Li et al., 2014; Li et al., 2021; Li et al., 2022; Manning et al., 2009; Pettigrew et al., 2005). The WMCC is both weaker and broader than the EMCC and is often described as being comprised of both an inshore and offshore core (Li et al., 2022). The inshore core is primarily driven by river runoff, especially from the Penobscot and Kennebec-Androscoggin rivers (Li et al., 2022). The offshore branch of the WMCC is primarily supplied by the extension of the EMCC (Li et al., 2022) and is more influenced by the connectivity to the EMCC than its inshore counterpart.

The GMCC system advects nutrients, larvae and dinoflagellates (including the toxic *Alexandrium Fundyense*) throughout the GOM (Anderson et al., 2005; Brooks & Townsend, 1989; Churchill et al., 2005; Huret et al., 2007; Li et al., 2014), creating the possibility of population connectivity between distant locations along the coast. As such, the overall flow of the GMCC and the connectivity between its branches have important ecological consequences for the region. Even the most economically valuable species in the GOM, *Homarus Americanus* (lobster) has been shown to be impacted by the state of the GMCC: in years when the EMCC veers offshore (i.e., connectivity between the branches is low and flow in the WMCC is reduced), retention of planktonic lobster larvae south of the bifurcation point increases (Xue et al., 2008). In other words, weak WMCC transport has been linked to conditions favorable to lobster recruitment southwest of Penobscot Bay. Clearly, a better understanding

of the long-term variability in the GMCC system and how the system is likely to respond to changing climate conditions within the GOM is desirable.

Variability in the GMCC on seasonal and short inter-annual time periods has been studied in the past (Brooks, 1994; Chen et al., 2006; Churchill et al., 2005; Feng et al., 2016; Li et al., 2014; Li et al., 2021; Li et al., 2022; Lynch et al., 1997; Xue et al., 2000) and three mechanisms have been used to explain changing transport by the system: (a) changes in the intensity of the geostrophic transport along the coast (b) changes in the intensity of the southwesterly winds in the region and (c) changes in the amount of river discharge flowing into the GOM. Mechanisms 1 (changes to the geostrophic flow) and 2 (changes in the wind fields) were investigated in a shorter-term study focusing on inter-annual variability in the system between 2002 and 2011 (Li et al., 2014). First, the study linked a slowdown in the current in 2010 to the unusually large intrusion of Warm Slope Water (WSW) and fresher-than-usual Scotian Shelf Water (SSW) in that year (Li et al., 2014). This increase in warm and fresh water within the GOM led to a reduced dynamic height gradient across the interior GOM and thus slowed the geostrophic transport of the GMCC (Li et al., 2014). Second, the study noted that the year 2010 experienced southwesterly winds that, by inducing Ekman transport offshore, favored upwelling conditions in the region. By disrupting the southwestward flow of the current, these upwelling conditions also likely contributed to the reduction in the alongshore transport of the GMCC (this mechanism was also suggested in Churchill et al., 2005; Fong et al., 1997) in 2010. The third mechanism (river runoff) was investigated more recently: in their 2022 work Li et al. examined changes in the amount of river discharge from the rivers emptying into the GOM. They noted that the WMCC appeared to be particularly susceptible to changes in the Penobscot and Kennebec-Androscoggin outflow. When anomalously large river discharge was observed, Li et al. noted an increased flow in the downstream WMCC.

Unfortunately, as global temperatures rise, the GOM is experiencing unprecedented levels of warming (Pershing et al., 2015; Pershing et al., 2021) which has made predicting the nature of the GMCC in future climate scenarios difficult. The warming experienced by the GOM to date far exceeds the level of warming noted in most regions of the global ocean (Pershing et al., 2015) and has the potential to alter the physical characteristics of the GOM (Brickman et al., 2021) and the ecosystems that thrive within it (Pershing et al., 2021). The impact of this warming on the GMCC remains unclear. On the one hand, WSW influences that Li et al. (2014) linked to decreased transport of the GMCC have become increasingly common in the GOM in the last 10–15 years (Brickman et al., 2018; Friedland et al., 2020; Galbraith et al., 2019; Hebert et al., 2018). On the other hand, the increasing number and intensity of storm events in the GOM (whose northeasterly winds would favor shoreward Ekman transport and increased transport by the WMCC) (Li et al., 2022) may yield the opposite change. Uncertain precipitation patterns may also lead to variability in the strength of the river discharges in the region. Model results presented in Brickman et al. (2021) highlight the difficulty of predicting GOM circulation changes: the Bedford Institute of Oceanography North Atlantic Model (BNAM) simulations (Brickman et al., 2016; Brickman et al., 2018; Wang et al., 2019) project a *decreased* counterclockwise circulation within the GOM in future years while the Regional Ocean Modeling System (ROMS) (Kang & Curchitser, 2013; Shchepetkin & McWilliams, 2003; Shchepetkin & McWilliams, 2005) projections (Alexander et al., 2020) suggest that the counterclockwise circulation of the GOM will *increase* with warming temperatures.

No long-term analysis has yet been completed to determine whether and how changing oceanographic conditions in the GOM have affected the flow of the GMCC on inter-decadal timescales. Here, we use data collected by Lagrangian drifters in the GOM, long-term velocity and wind data from the Northeast Regional Association of Coastal Ocean Observing Systems (NERACOOS) buoy arrays within the GMCC and river discharge data from the United States Geological Survey (USGS) to determine whether and how the GMCC system has changed on inter-decadal timescales. A better understanding of how the current has changed to date may help scientists to better prepare for future changes in the GOM.

2. Data and Methodology

2.1. Drifter Dataset: Calculation of Current Velocities From Lagrangian Drifters

The Lagrangian drifter dataset analyzed in this study overlaps the drifter dataset presented in Manning et al. (2009), which utilized drifters that entered the GOM between 1988 and 2007. The construction, operation and reliability of the drifters are well described in the Manning et al. study, so are only briefly summarized here. Surface drifters included in this study primarily consisted of a vertical mast holding a set of four vinyl sail cloths

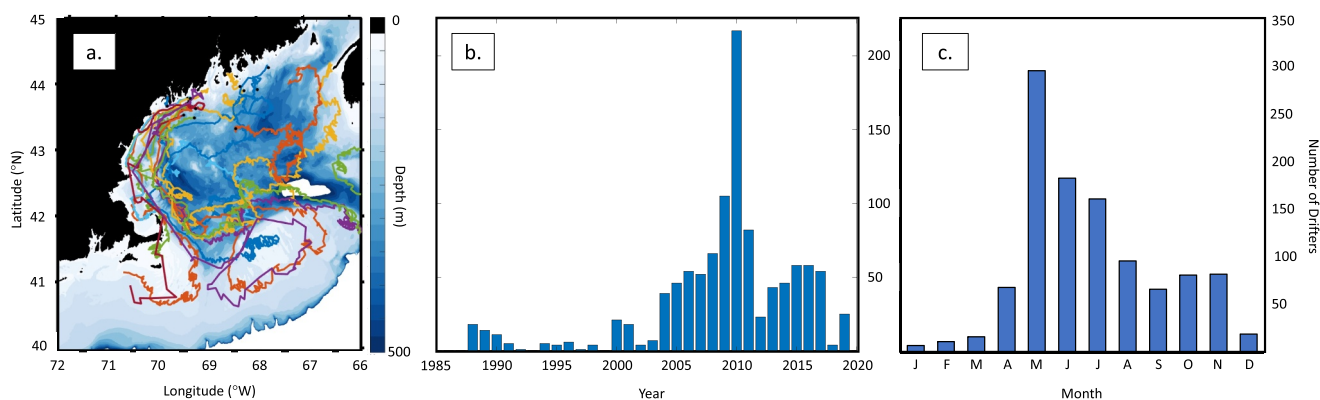


Figure 2. (a) 20 sample trajectories shown over Gulf of Maine bathymetry (0–500 m). The trajectories shown in this figure were all from the year 2000. Each trajectory is shown in a different color. Small black dots depict the launch location for each drifter. (b) Number of drifters launched in the GOM by year (c) Number of drifters launched in the GOM by month.

below the surface. The masts were ballasted to minimize exposure above the surface. A GPS antenna located on the top of the unit transmitted data to satellites at various time-intervals depending on the needs of the scientists involved in specific drifter launches. A small number of drifters in the dataset also had drogues that centered in the top 15 m of the water column. The treatment of the drogued drifters is described in more detail below.

Drifter data was extracted from the National Oceanic and Atmospheric Administration's (NOAA) Northeast Fisheries Science Center's ERDDAP website (comet.nfsc.noaa.gov/erddap/tabledap/floaters.html). Latitude, longitude and date data were examined for 1,091 drifters that entered the GOM between 1988 and 2019. Most of the drifters were launched during the two decades that will be the main focus of this work: 2000–2009 (412 drifters) and 2010–2019 (648 drifters). 5 of the drifters recorded tracks that were too short for inclusion in this work, so 1,086 drifter tracks were ultimately analyzed. The majority of drifters were launched in the spring and summer months ($N = 37$ for winter (DJF), $N = 380$ for spring (MAM), $N = 440$ for summer (JJA) and $N = 229$ for fall (SON)). Sample drifter tracks (2a) as well as the number of drifters launched per year (2b) and per month (2c) are shown together in Figure 2.

In order to produce velocity plots from the drifter dataset, the drifters were first quality controlled by removing points with unrealistic velocities, following the procedure set forth in Hansen and Poulain (1996). The raw drifter data was then used to calculate drifter velocities along the drifter path at 6 hr time intervals. European Centre for Medium-Range Weather Forecasts (ECMWF) wind fields (6 hr resolution) were used to calculate the likely slippage of drifters due to the wind at each 6 hr fix. The calculated slippage was removed from each 6 hr drifter fix using a procedure based on the one set forth in Laurindo et al. (2017). The downwind slip coefficient for the undrogued drifters was estimated to be 5.85×10^{-3} , which is the middle of the range put forth for the GOM in the Laurindo et al. study. A downwind slip coefficient of 7×10^{-4} was used for the drogued drifters (Niiler et al., 1995). When appropriately corrected for the wind slippage, velocity estimates gathered by drogued and undrogued drifters are virtually identical (Laurindo et al., 2017). Therefore, data gathered from both drogued and undrogued drifters are included in the dataset analyzed in this study. Once the wind slippage had been subtracted from the interpolated velocities, velocities were low pass filtered following the technique in Lumpkin and Johnson (2013), using a fifth order Butterworth filter with a cutoff period of 23.5 hr (1.5 times the local inertial period at 45°N). Finally, the resultant velocities were averaged to create daily values (days with only one six-hour interpolated velocity recorded were removed) and then bin averaged using a bin size of 0.25°. The velocity plot put together incorporating data across all available years (1988–2019) can be seen in Figure 3. Velocity plots broken into two individual decades (2000–2009 and 2010–2019, the decades where sufficient drifter coverage was available within the GOM) are shown together in Figure 4. The number of filtered daily fixes averaged in each 0.25° bin to produce the decadal velocity fields are shown in Figure 5. As evident in Figures 3 and 4, the surface drifter dataset sufficiently resolves the major features of the GOM circulation, including the cyclonic circulation within the GOM, the anticyclonic circulation around George's Bank and the bifurcation of the GMCC offshore of Penobscot Bay.

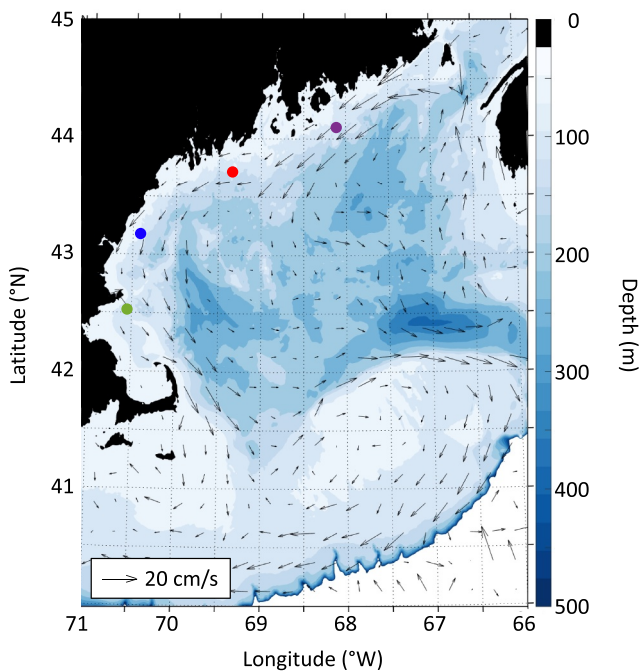


Figure 3. Mean velocities calculated from the combined drifter dataset from 1988 to 2019. Locations of the NERACOOS buoys A01 (green), B01 (blue), E01 (red) and I01 (purple) are shown. Bathymetry shaded in blue represents depths from 0 to 500 m.

2.2. NERACOOS Buoy Dataset: Calculation of Current Velocities From Fixed Buoys

The velocity fields calculated from the drifter trajectories were supplemented with and compared to long-term records of current velocities from the NERACOOS buoy array (now available on the NERACOOS Mariner's Dashboard at <https://mariners.neracoos.org>). Current speed and direction (hourly resolution) were downloaded from NERACOOS buoys A01 (Massachusetts Bay), B01 (Western Maine Shelf), E01 (Central Maine Shelf) and I01 (Eastern Maine Shelf) for three different depths (2, 10 and 50 m) for the period of January 2001–December 2021 (locations of the four buoys are shown as colored dots in Figures 3, 4 and 6). The alongshore velocity was calculated for each buoy over the course of the timeseries at daily and monthly resolutions. The coastline angles used to calculate “alongshore” flow varied depending on the local orientation of the coastline. Coastline angles relative to due north were determined to be 170.88° (A01), 217.12° (B01), 249.50° (E01) and 238.81° (I01). Best-fit linear trends were identified using linear regression and trends with a p-value less than 0.05 were deemed significant. Seasons were defined in the same manner as specified in Section 2.1.

2.3. NERACOOS Buoy Dataset: Calculation of Wind Speed Over the GOM

Wind speed and direction (hourly resolution) were also downloaded from the NERACOOS buoys for the period 2001–2021. Since the southwesterly character of the winds is of particular interest in the GOM region (southwesterly winds were previously linked to upwelling which disrupted the GMCC flow (Churchill et al., 2005; Fong et al., 1997)), the winds were projected onto 225° (winds blowing from the southwest). A moving average filter across five datapoints was used to smooth the data and a local linear regression technique, LOWESS (locally weighted scatterpoint smoothing), was applied. Wind

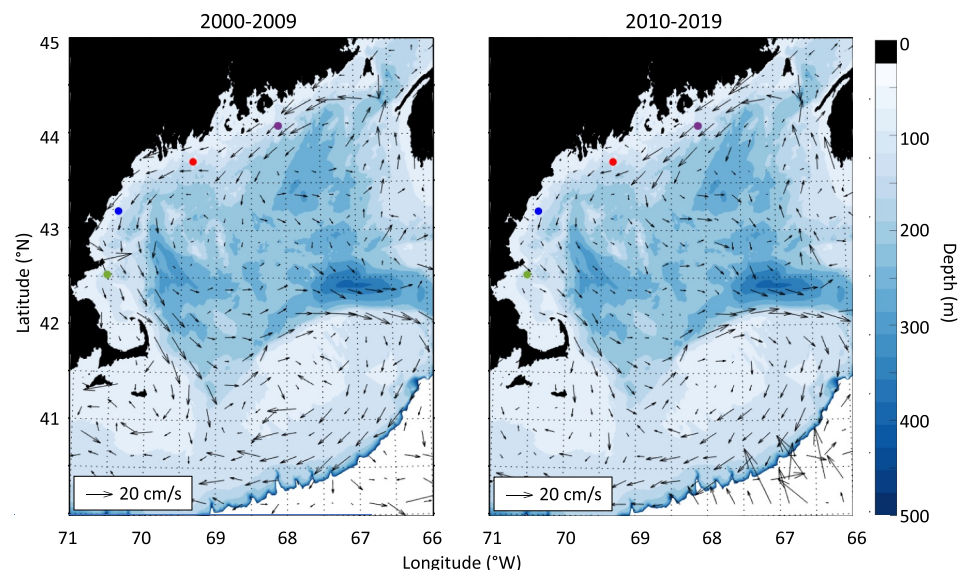


Figure 4. Drifter-derived velocities from the period 2000–2009 (left) and 2010–2019 (right). Locations of the NERACOOS buoys A01 (green), B01 (blue), E01 (red) and I01 (purple) are shown. Bathymetry shaded in blue represents depths from 0 to 500 m.

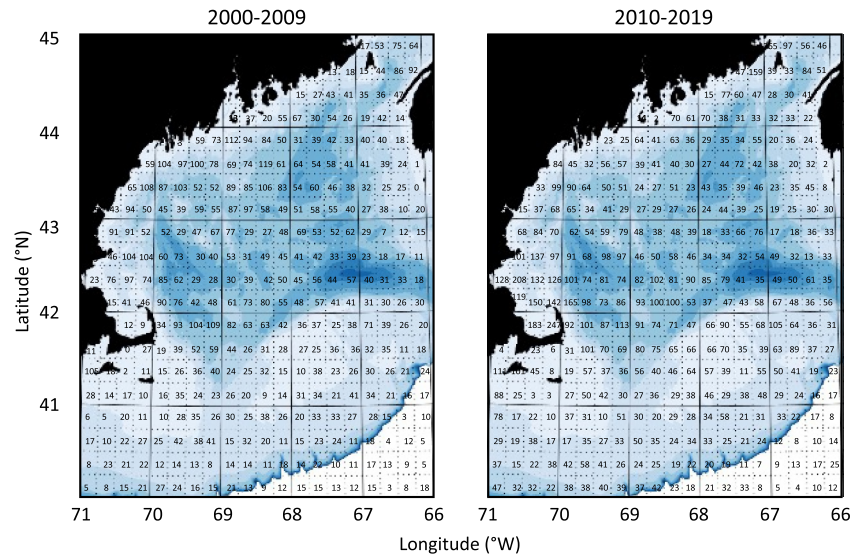


Figure 5. Number of filtered daily averaged fixes recorded by drifters in 0.25° bins during the period 2000–2009 (left) and 2010–2019 (right).

speeds that fell outside of six mean absolute deviations were removed. Positive trends in the projected wind fields in this analysis indicate a strengthening of the winds from the southwest. As with the NERACOOS buoy data, best-fit linear trends were identified using linear regression and deemed significant for p -values less than 0.05.

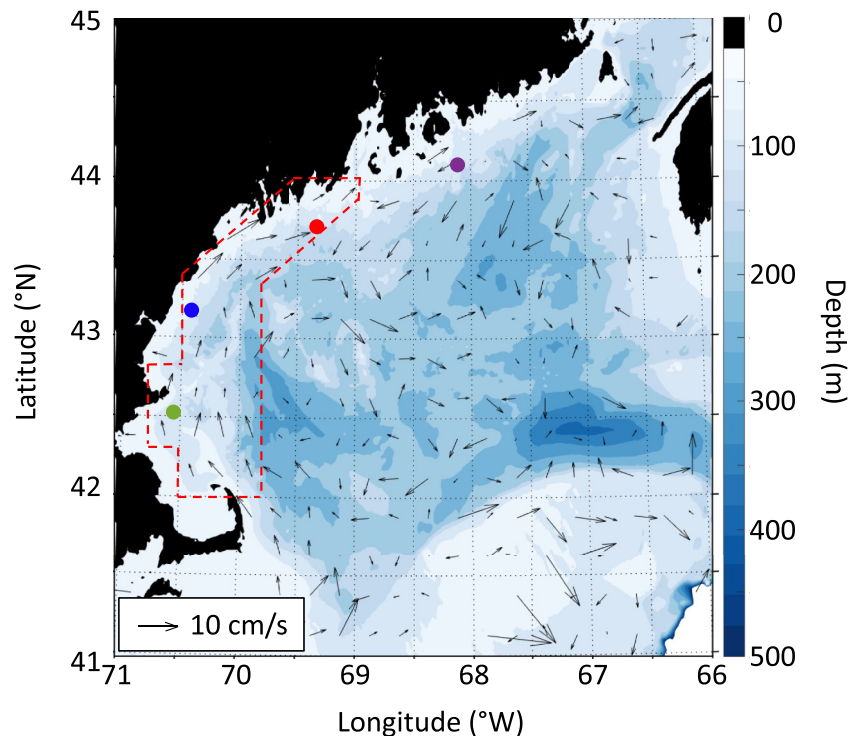


Figure 6. Velocity anomalies calculated from the drifter dataset (2010s–2000s). Colors indicate the locations of NERACOOS Buoys A01 (green), B01 (blue), E01 (red) and I01 (purple). The red dotted line denotes the velocity anomalies that were included when calculating the average slowdown in the region of the WMCC from the drifter-derived velocity fields. Bathymetry shaded in blue represents depths from 0 to 500 m.

2.4. River Discharge Calculations

Monthly average river discharge data (m^3/s) for the Androscoggin, Saco, Penobscot, and Kennebec Rivers was downloaded from the USGS National Water Information System web interface for the period spanning January 2000–December 2020 (waterdata.usgs.gov). No discharge data was available for the Kennebec River until after September 2000, so the Kennebec River discharge analysis was limited to 2001–2020. In river systems where multiple stations were available to report data, the station closest to the coast was selected and utilized. Linear trends in the river discharge were calculated and trends were considered significant when p -values were less than 0.05.

3. Results

3.1. Long-Term Changes in GMCC Velocities: Deductions From Drifters

The velocity fields produced from the Lagrangian drifter dataset capture many of the major features of the GOM circulation (Figures 3 and 4). Specifically, at 0.25° resolution the mean (Figure 3) and decadal (Figure 4) velocity fields calculated from the drifters show cyclonic circulation around the GOM, the bifurcation of the flow of the GMCC, flow into the Great South Channel, and the anticyclonic circulation around George's Bank. The velocities in the GMCC apparent in the Lagrangian analysis are roughly consistent with those found elsewhere in the literature: velocities in the EMCC have been reported at 10–16 cm/s and slow in the region of the WMCC (Li et al., 2021; Li et al., 2022; Manning et al., 2009).

In order to understand how the GOM is changing on inter-decadal timescales, the velocities calculated from drifters for the years 2000–2009 were subtracted from the velocities from the period 2010–2019 in $1/4^\circ$ boxes throughout the GOM region. Grid boxes with fewer than 20 daily fixes contributing to the average velocity for that grid were not included. The interdecadal differences in the velocity fields between the 2000s and the 2010s can be seen in Figure 6. Though a number of interesting features can be observed in the difference plot, the slowdown of the GMCC, particularly in the WMCC region of the current system, is the most readily apparent feature. The velocities west and north of the Wilkinson Basin (labeled in Figure 1) appear to have slowed significantly over the time period of interest (Figure 6), with a maximum slowdown of 9.6 cm/s per decade. The average slowdown in the region of the WMCC (calculated using the velocity anomalies within the red dotted line in Figure 6) was 4.9 cm/s per decade. In the sections that follow, we aim to determine whether this multi-decadal slowdown is apparent in other (Eulerian) measurements of the current over similar time periods (Section 3.2) and then investigate a number of potential drivers for this change (Sections 3.3–3.5).

3.2. Long-Term Changes in GMCC Velocities: Deductions From NERACOOS Buoys

The data presented in Section 3.1 points to an apparent slowdown in the surface waters of the GMCC over long time periods, particularly in the region of the WMCC. In this section, velocity changes collected within the Eulerian frame at fixed buoy locations are introduced in order to test for consistency of the signal across the two datasets and to quantify the magnitude of the slowdown at fixed locations. Furthermore, the use of NERACOOS

buoy data allows us to compare the surface water changes observed by the drifters with changes at deeper depth levels. The multi-decadal trends observed at 2, 10 and 50 m depths at each of the four buoy locations are shown together in Table 1. As evident in Table 1, the slowdown observed in the drifter record is largely consistent with the anomalies calculated from the surface drifter data. At 2 m depth, a statistically significant slowdown was observed at Buoys B01 and E01 (Figures 7a and 7b), which are located in the region predicted by the drifter dataset to experience a strong slowdown. A surface water slowdown was also predicted at Buoys I01 and A01, though the trend in those locations did not yield statistical significance. The slowdown trend observed at Buoys B01 and E01 weakens with depth and is no longer statistically significant at 50 m.

To better understand the changes in the NERACOOS buoy velocity fields, the changes in the 2 m velocity fields (where the slowdown trend is the strongest) were further broken down by season in Table 2. As evident in Table 2, the

Table 1
Long Term (2001–2021) Changes in Alongshore Velocities From NERACOOS Buoys at 2, 10 and 50 m Depth, Separated by Buoy Location

Long term changes in alongshore velocities (cm/s per decade)			
Buoy	2 m	10 m	50 m
A01	−0.330	−0.099	0.020
B01	−2.065	−0.527	0.306
E01	−1.100	−0.655	−0.254
I01	−0.018	0.231	0.356

Note. Velocity changes are reported in cm/s per decade. Negative values indicate a reduction in the alongshore transport. Changes with slopes that are significant at the $p > 0.05$ level are shown in bold. Statistically significant slowdowns are highlighted in red.

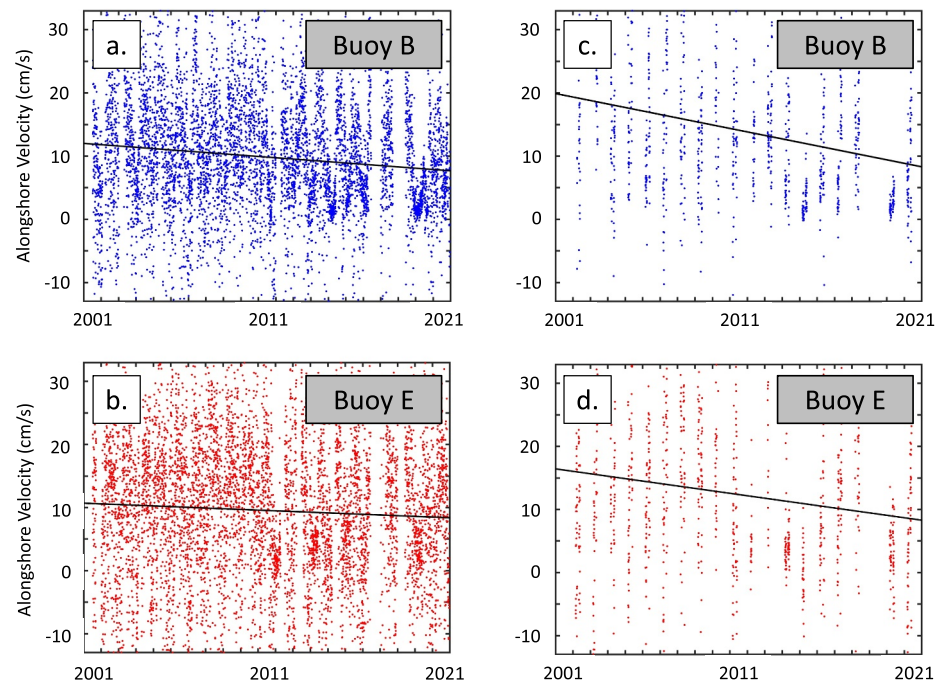


Figure 7. Representative alongshore velocities at Buoy B01 (top) and Buoy E01 (bottom) at 2 m depth. Panels on the left (a) and (b) include all data and panels on the right (c) and (d) include only spring (MAM) velocities. Positive alongshore velocities indicate flow along the coastline toward the southwest.

strongest slowdowns in the 2 m velocity fields occurred in spring at Buoys B01 (5.5 cm/s per decade, Figure 7c) and E01 (4.3 cm/s per decade, Figure 7d). The magnitude of these slowdowns are broadly consistent with the estimates of the slowdowns derived from the Lagrangian drifters (which are launched primarily in spring and summer): the average slowdown recorded by the drifters was 4.9 cm/s per decade.

In the sections that follow, potential causes of the GMCC slowdown over multi-decadal time periods are investigated. Specifically, each of the three mechanisms previously linked to interannual changes in GMCC transport will be examined on longer timescales: in Section 3.3, changes to the geostrophic flow field are discussed (mechanism 1), followed by changes in the winds over the GOM (mechanism 2, Section 3.4), and changes to river outflows in the region (mechanism 3, Section 3.5).

3.3. Changes in the Geostrophic Flow of the GMCC

As described in Section 1, changes in sea surface height (SSH) within the GOM have been linked to changes in the geostrophic flow of the GMCC in the past (Li et al., 2014). Subsurface temperature records from NERACOOS Buoy M (located in the interior GOM, not shown) confirm that subsurface temperatures in the interior have increased in the long term, a fact that has been well documented (e.g., Morrison et al., 2012). In theory, the presence of warmer waters in the GOM interior could have contributed to the observed surface water slowdown in the GMCC by elevating the mid-basin SSH, reducing the SSH gradient across the GMCC, and slowing the GMCC flow as a whole. However, it is clear from the NERACOOS buoy results presented in Section 3.2 that the changes observed in the GMCC since 2000 are primarily restricted to the surface waters. It is therefore unlikely that the observed surface water slowdown over long time periods would be due to a change in the geostrophic flow, which would be expected to impact both the surface and the subsurface flow fields.

Table 2
Long Term (2001–2021) Changes in Alongshore Velocities From NERACOOS Buoys at 2 m Depth, Separated by Season and Buoy Location

Long term changes in alongshore velocities (cm/s per decade) at 2 m depth by season

Buoy	Spring	Summer	Fall	Winter	Overall
A01	−1.142	0.151	−0.672	−0.109	−0.330
B01	−5.470	−2.202	−0.840	−0.720	−2.065
E01	−4.256	0.379	−0.503	0.107	−1.100
I01	−1.189	0.280	−1.375	1.917	−0.018

Note. Velocity changes are reported in cm/s per decade. Negative values indicate a reduction in the alongshore transport. Changes with slopes that are significant at the $p > 0.05$ level are shown in bold. Statistically significant slowdowns are highlighted in red.

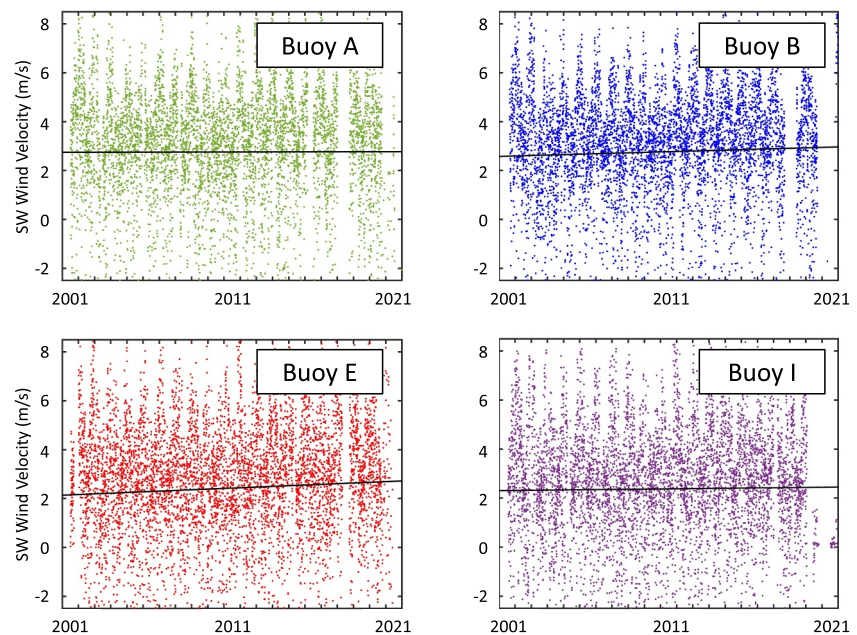


Figure 8. 10 m wind field data projected onto 225° at Buoy A01 (green), B01 (blue), E01 (red) and I01 (purple). Positive values indicate winds blowing to the northeast from the southwest. Black lines indicate the linear trend at each station.

3.4. Changes in the GOM Winds

The wind fields over the GOM are characterized by strong flow from the northwest in winter and weaker winds from the southwest in the summer (Xue et al., 2000). Since the disruption of the GMCC flow has previously been linked to an increase in winds from the southwest on shorter timescales (Fong et al., 1997; Churchill et al., 2005), the winds in this study were projected onto 225° (winds blowing from the southwest) in order to determine whether the southwesterly component of the winds had increased or decreased on inter-decadal timescales.

The long-term trends in the 10 m wind fields observed at Buoy A01, B01, E01 and I01 (Figure 8) are shown together in Table 3. As evident in Table 3, a statistically significant strengthening of the southwesterly winds was observed at 2 of the 4 NERACOOS stations (B01 and E01) over the time period of interest. Importantly, the two buoys that experienced the most significant strengthening of the winds also experienced the most significant slowdown in the alongshore flow of the surface waters (B01 and E01). The largest change in the wind fields was observed at Buoy E01, where the southwesterly winds increased at a rate of 27.8 cm/s per decade. Pearson correlation coefficients relating the raw (unsmoothed) wind strength data to the 2 m velocities at Buoy B01 and E01 indicate moderate but statistically significant inverse correlations between the two timeseries (-0.41 ($p < 0.01$) and -0.44 ($p < 0.01$) respectively). Therefore, we conclude that it is possible that over long time periods, strengthening southwesterly winds may have contributed to the observed slowdown in the GMCC, particularly in the region of the WMCC. Trends at Buoy A01 and Buoy I01 also showed increases in wind strength at a smaller rate, though the trends in those locations were not statistically significant (Table 3). It is perhaps unsurprising then, that changes in the current velocity at those locations were also insignificant.

Table 3

Long Term (2001–2021) Changes in the Southwesterly Component of the Winds Over Buoy A01, B01, E01 and I01

Long term changes in southwesterly component of winds over NERACOOS buoys		
Buoy	Overall (cm/s per decade)	Pvalue
A01	1.1	0.86
B01	18.5	<0.01
E01	27.8	<0.01
I01	6.8	0.29

Note. Positive values indicate a strengthening of the southwesterly component of the winds. Locations with a statistically significant strengthening of the winds are shown in red.

3.5. Changes in the River Runoff

The outflows of the Penobscot and Kennebec-Androscoggin (K-A) rivers have been found to be particularly impactful on the flow of the WMCC (Li et al., 2022). However, river discharge data collected at sites in the Androscoggin, Kennebec, Saco and Penobscot rivers between 2000 and 2020 (Figure 9) do not support the idea that changes in river discharge has been responsible for the observed GMCC slowdown over long time periods. No

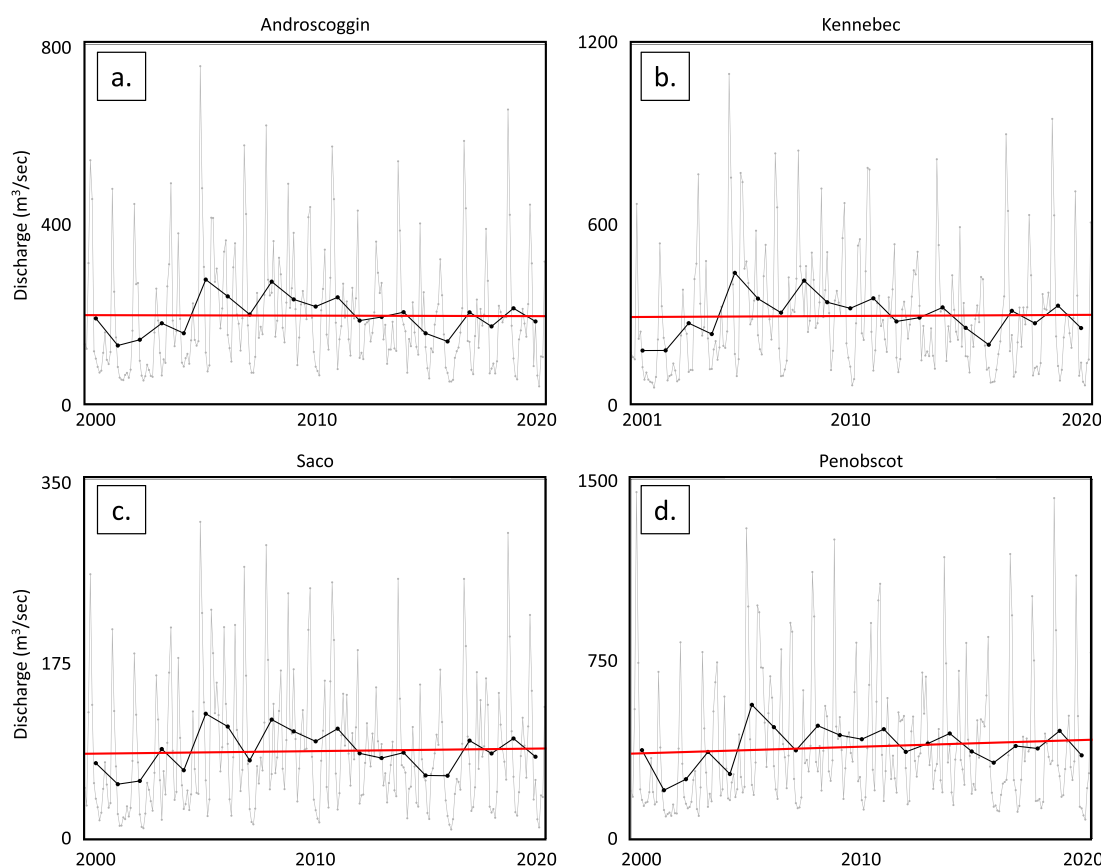


Figure 9. River Discharge from (a) Androscoggin, (b) Kennebec, (c) Saco and (d) Penobscot rivers through time. Discharge has been shown to be increasing through time for all sites except for the Androscoggin. However, none of the trends in river discharge reached statistical significance.

statistically significant changes in river discharge were observed in any of the four rivers examined in this work over the time period of interest. Furthermore, though the trends was not significant, in three of the four river discharge records discharge *increased* over the time period of interest (2000–2020): the Kennebec ($0.36 \text{ m}^3/\text{s}$ per year), the Saco ($0.25 \text{ m}^3/\text{s}$ per year) and the Penobscot ($2.77 \text{ m}^3/\text{s}$ per year). Only the Androscoggin River showed a slight decrease in discharge over the time period of interest ($-0.11 \text{ m}^3/\text{s}$ per year) and the magnitude of the decrease was small relative to the increases observed in the other rivers. As such, long term changes in the river outflow are unlikely to have caused the observed surface water slowdown in the WMCC.

4. Discussion

4.1. The Long-Term Slowdown in the GMCC Surface Waters

The complex nature of the GMCC system is apparent in this work. The use of both Lagrangian and Eulerian datasets to examine the current has allowed for a comprehensive look at both its mean state and its long-term changes. In the mean, the datasets both depict a current consistent with the image previously depicted in the literature: a strong EMCC that divides off the coast of Penobscot into a weaker WMCC and a flow to the GOM interior. Here, we present new findings that are consistent across the Lagrangian and Eulerian datasets: the GMCC has experienced an overall slowdown in its surface waters, particularly in the region of the WMCC. The strength of the slowdown was measured by the NERACOOS moorings to be $\sim 1\text{--}2 \text{ cm/s}$ per decade since the early 2000s overall and up to 5.5 cm/s per decade in the spring. The slowdown measured by the drifters (which were most commonly launched in the spring and summer) in the region of the WMCC averaged 4.9 cm/s per decade.

Short-term variability in the WMCC has been linked to a variety of factors, including changes in the south-westerly winds (Li et al., 2014), changes in the geostrophic flows in the region (Li et al., 2014) and changes in the discharge from rivers that supply the WMCC (Li et al., 2021). However, long term examinations of each of these

factors over two decades revealed that neither changes to geostrophic flows nor long-term changes in river discharge could explain the observed slowdown within the surface waters of the GMCC on inter-decadal timescales. Only the increase in the strength of the southwesterly winds over the GOM on long timescales (Figure 8) is consistent with the observed slowdown. As such, we conclude that the long-term surface water slowdown has likely been driven thus far by the local disruption of the flow by the increasingly strong southwesterly winds, as hypothesized by others on shorter timescales (Churchill et al., 2005; Fong et al., 1997; Li et al., 2014).

Interestingly, a recent paper by Scully et al. (2022) included a record of long-term winds recorded at the Boston Buoy 44013, located 16 nautical miles east of Boston (slightly to the southwest of Buoy A01, analyzed in this study). In that location, the authors demonstrate (and our subsequent analysis using the techniques described in this study confirm) that the long-term winds from the southwest have been *decreasing* over time rather than increasing, as we see at the nearby Buoy A01. No long term current data is available from the Boston Buoy, so it is impossible to investigate potential changes to the surface flows over the same time period at the location of the Boston Buoy directly. However, certainly the differences in the winds between Buoy A01 and the Boston Buoy highlight the complexity of the region south of Cape Ann. It is possible that this complexity contributed to the relatively weak trend we see in the current at Buoy A01 relative to stations located further north. A more in depth analysis of the temporal and spatial changes in the GOM wind fields over long time periods would be worthwhile.

Finally, the findings of this work do not preclude the possibility that future long-term trends in geostrophic flows or river discharges could impact the long-term flow of the WMCC. Rather, we suggest here that *to date* the only forcing mechanism consistent with the observed long-term surface water slowdown is the strengthening of the southwesterly winds.

4.2. What's Next for the WMCC?

As described in Section 1, the impact of a warming climate on the GMCC is unclear in model studies. In fact, Brickman et al. (2021) highlight the relative difficulty of predicting future circulation changes relative to other scalar variables such as temperature and salinity. This difficulty has manifested itself in contradictory results from different models: the ROMS model predicts that the overall cyclonic circulation of the GOM will be enhanced in future years while the BNAME model suggests the cyclonic flow will decrease (Brickman et al., 2016). In both cases, the observed changes in the model may have been linked to changes in the transport of waters into the GOM via the NEC and Nova Scotia Current (NSC), a process that would be governed by basin-scale, rather than regional-scale, climate forces. The authors note that the changes in transport predicted by the models are small in most places (<5%) but their work serves as a reminder that the GOM system is a part of a larger whole that is itself changing (Brickman et al., 2016). Though changes in the geostrophic flow were not found to be a major driver of changes in the GMCC surface flow to date, changes in the transport of waters into the GOM as larger Atlantic-scale changes take place in the future could certainly impact the nature of the flow within the GOM in the years to come.

The complex dynamics involved in predicting long-term trends in winds make predicting the likely changes to winds in the GOM difficult going forward. Variability in wind speed and direction is often related to both local and regional forcings. Natural variability in winds can extend on time periods that last a decade or longer. However, a recent analysis of long-term changes in wind fields has indicated that the recent intensification of winds observed at the NERACOOS buoys is likely to continue for at least the next decade (Zeng et al., 2019). If this intensification persists in the GOM, it is possible that the disruption to the flow of the GMCC may continue and, unless offset by other changes, the slower velocities experienced in the last decade may become the norm for the surface waters of the region.

Rain in the GOM region has been increasing over long time periods. In Maine, the average annual precipitation has increased by 15% since 1895 (Fernandez et al., 2020). The impact of this additional rain may be expected to lead to increased river discharge and stronger GMCC velocities. Over the time period of interest in this study (2000–2020), these trends were not observed; river discharge rates did not change significantly and GMCC velocities slowed. However, if the overall amount of discharge significantly increases in the future, the impact of the additional discharge may buffer some of the observed slowdown resulting from the intensifying southwesterly winds.

4.3. Potential Impact of the GMCC Surface Water Slowdown on the Ecosystems of the GOM

A long-term change in the nature and speed of the GMCC surface flow could have far-reaching consequences for life within and around the GOM. Though examining the full extent of the potential changes goes beyond the scope of this work, it is worth noting that the changes observed in the GMCC circulation (an overall slowdown, particularly in the region of the WMCC) may be consistent with an increase in the overall population of lobster in the GOM in recent years. As pointed out in Xue et al. (2008), in times when the GMCC connectivity is low (and the transport by the WMCC is small), retention of planktonic lobster in the region of the WMCC increases. Though the overall increase in the GOM lobster population in recent decades likely has many contributing factors (including increases in bottom temperatures in the region), the slowdown in the GMCC surface waters may have played a role in creating conditions favorable for population growth. The potential ecological and economic consequences of a continued slowdown should be examined in future work.

Data Availability Statement

The data analyzed in this study is publicly available. Drifter data was extracted from NOAA's Northeast Fisheries Science Center's ERDDAP website (comet.nefsc.noaa.gov/erddap/tabledap/drifters.html). Historical NERACOOS data (for both wind and currents) is available via the NERACOOS graphing and download tool: https://www3.neracoos.org/lg/gnd/if_index.html. The variables downloaded for this study were current speed and direction (at 2, 10 and 50 m) and wind speed and direction for buoys A01, B01, E01 and I01. The monthly average river discharge data is available at the USGS National Water Information System web interface: <https://dash-board.waterdata.usgs.gov/app/nwd/en/>. To access historical discharge data at a particular site, use the search function to easily locate stations on a particular river (enter the name of the river in the search field). When the "suggested sites" pop up window appears, select the "USGS Station: Surface Water" record at the station of interest. Click on the station of interest on the map. Once the site is selected, click on the data tab and then the "monthly statistics" link to access monthly averaged discharge data. The stations selected for this work were the stations located closest to the coast that contained historic discharge data for each river.

Acknowledgments

Many of the drifters analyzed in this study were launched as part of the Student Drifter Program (SDP, www.studentdrifters.org) which has been run for many years by the combined efforts of Jim Manning (NOAA, retired, a co-author on this study) and Erin Pelletier (Gulf of Maine Lobster Foundation). The authors gratefully acknowledge the importance of the SDP in both providing valuable data and building community. We thank the schools (more than 100!) involved with building drifters in the classroom and the dozens of fishermen who made deployments as part of the SDP. K.B. also gratefully acknowledges financial support from Maine Sea Grant and the combined contributions of the many Stonehill College undergraduate research students whose work advanced the early stages of this project. Finally, the authors acknowledge the helpful comments of the anonymous reviewers whose insights strengthened this manuscript.

References

- Alexander, M. A., Shin, S.-I., Scott, J. D., Curchitser, E., & Stock, C. (2020). The response of the Northwest Atlantic Ocean to climate change. *Journal of Climate*, 33(2), 405–428. <https://doi.org/10.1175/JCLI-D-19-0117.1>
- Anderson, D. M., Stock, C. A., Keafer, B. A., Nelson, A. B., Thompson, B., McGillicuddy Jr, D. J., et al. (2005). Alexandrium Fundyense cyst dynamics in the Gulf of Maine. *Deep Sea Research Part II: Topical Studies in Oceanography*, 52(19–21), 2522–2542. <https://doi.org/10.1016/j.dsr2.2005.06.014>
- Bigelow, H. B. (1927). Physical oceanography of the Gulf of Maine. *Fisheries Bulletin*, 40, 511–1027.
- Brickman, D., Alexander, M. A., Pershing, A., Scott, J. D., & Wang, Z. (2021). Projections of physical conditions in the Gulf of Maine in 2050. *Elementa Science of the Anthropocene*, 9(1), 00055. <https://doi.org/10.1525/elementa.2020.20.00055>
- Brickman, D., Hebert, D., & Wang, Z. (2018). Mechanism for the recent ocean warming events on the Scotian Shelf of eastern Canada. *Continental Shelf Research*, 156, 11–22. <https://doi.org/10.1016/j.csr.2018.01.001>
- Brickman, D., Wang, Z., & DeTracey, B. (2016). High resolution future climate ocean model simulations for the Northwest Atlantic Shelf Region. *Canadian Technical Report of Hydrography and Ocean Sciences*, 315. xiv + 143.
- Brooks, D. A. (1994). A model study of the buoyancy-driven circulation in the Gulf of Maine. *Journal of Physical Oceanography*, 24(11), 2387–2412. [https://doi.org/10.1175/1520-0485\(1994\)024<2387:amsotb>2.0.co;2](https://doi.org/10.1175/1520-0485(1994)024<2387:amsotb>2.0.co;2)
- Brooks, D. A., & Townsend, D. W. (1989). Variability of the coastal current and nutrient pathways in the eastern Gulf of Maine. *Journal of Marine Research*, 47(2), 303–321. <https://doi.org/10.1357/002224089785076299>
- Chen, C., Beardsley, R. C., & Cowles, G. (2006). An unstructured grid, finite-volume coastal ocean model (FVCOM) system. *Oceanography*, 19(1), 78–89. <https://doi.org/10.5670/oceanog.2006.92>
- Churchill, J. H., Pettigrew, N. R., & Signell, R. P. (2005). Structure and variability of the Western Maine Coastal Current. *Deep-Sea Research, Part II*, 52(19–21), 2392–2410. <https://doi.org/10.1016/j.dsr2.2005.06.019>
- Feng, H., Vandemark, D., & Wilkin, J. (2016). Gulf of Maine salinity variation and its correlation with upstream Scotian Shelf currents at seasonal and interannual time scales. *Journal of Geophysical Research: Oceans*, 121(12), 8585–8607. <https://doi.org/10.1002/2016JC012337>
- Fernandez, I., Birkel, S., Schmitt, C., Simonson, J., Lyon, B., Pershing, A., et al. (2020). *Maine's climate future 2020 update*. University of Maine. climatechange.umaine.edu/climate-matters/maines-climate-future/
- Fong, D. A., Geyer, W. R., & Signell, R. P. (1997). The wind-forced response on a buoyant coastal current: Observations of the western Gulf of Maine plume. *Journal of Marine Systems*, 12(1–4), 69–81. [https://doi.org/10.1016/S0924-7963\(96\)00089-9](https://doi.org/10.1016/S0924-7963(96)00089-9)
- Friedland, K. D., Morse, R. E., Manning, J. P., Melrose, D. C., Miles, T., Goode, A. G., et al. (2020). Trends and change points in surface and bottom thermal environments of the US Northeast Continental Shelf Ecosystem. *Fisheries Oceanography*, 29(5), 396–414. <https://doi.org/10.1111/fog.12485>
- Galbraith, P. S., Chasse, J., Caverhill, C., Nicot, P., Gilbert, D., Lefavre, D., & Lafleur, C. (2019). Physical oceanographic conditions in the Gulf of St. Lawrence during 2018. In *DFO Canadian Science Advisory Secretariat Document*. 2019/046. iv þ 79 p.
- Hansen, D. V., & Poulain, P. M. (1996). Quality control and interpolations of WOCE-TOGA drifter data. *Journal of Atmospheric and Oceanic Technology*, 13(4), 900–909. [https://doi.org/10.1175/1520-0426\(1996\)013<0900:qcaiw>2.0.co;2](https://doi.org/10.1175/1520-0426(1996)013<0900:qcaiw>2.0.co;2)

- Hebert, D., Pettipas, R., Brickman, D., & Dever, M. (2018). *Meteorological, sea ice and physical oceanographic conditions on the Scotian Shelf and in the Gulf of Maine during 2016*. DFO Canadian Science Advisory Secretariat (CSAS). 2018/016. v p 53 p.
- Huret, M., Runge, J., Changsheng, C., Cowles, G., Xu, Q., & Pringle, J. (2007). Dispersal modeling of fish early life stages: Sensitivity with application to Atlantic Cod in the Western Gulf of Maine. *Marine Ecology Progress Series*, 347, 261–274. <https://doi.org/10.3354/meps06983>
- Kang, D., & Curchitser, E. N. (2013). Gulf Stream eddy characteristics in a high-resolution ocean model. *Journal of Geophysical Research: Oceans*, 118(9), 4474–4487. <https://doi.org/10.1002/jgrc.20318>
- Laurindo, L. C., Mariano, A. J., & Lumpkin, R. (2017). An improved near-surface velocity climatology for the global ocean from drifter observations. *Deep Sea Research Part I: Oceanographic Research Papers*, 124, 73–92. <https://doi.org/10.1016/j.dsr.2017.04.009>
- Li, D., Wang, Z., Xue, H., Thomas, A. C., & Etter, R. J. (2022). Wind-Modulated Western Maine Coastal Current and its connectivity with the eEastern Maine Coastal Current. *Journal of Geophysical Research: Oceans*, 127(6), e2022JC018469. <https://doi.org/10.1029/2022jc018469>
- Li, D., Wang, Z., Xue, H., Thomas, A. C., Pettigrew, N., & Yund, P. O. (2021). Seasonal variations and driving factors of the Eastern Maine Coastal Current. *Journal of Geophysical Research: Oceans*, 126(11), e2021JC017665. <https://doi.org/10.1029/2021jc017665>
- Li, Y., He, R., & McGillicuddy Jr, D. J. (2014). Seasonal and interannual variability in Gulf of Maine hydrodynamics: 2002–2011. *Deep Sea Research Part II: Topical Studies in Oceanography*, 103, 210–222. <https://doi.org/10.1016/j.dsr2.2013.03.001>
- Lumpkin, R., & Johnson, G. (2013). Global ocean surface velocities from drifters: Mean, variance, ENSO response, and seasonal cycle. *Journal of Geophysical Research*, 118(2), 92–3006. <https://doi.org/10.1002/jgrc.20210>
- Lynch, D. R., Holboke, M. J., & Naimie, C. E. (1997). The Maine coastal current. *Continental Shelf Research*, 17(6), 605–634. [https://doi.org/10.1016/s0278-4343\(96\)00055-6](https://doi.org/10.1016/s0278-4343(96)00055-6)
- Manning, J. P., McGillicuddy Jr, D. J., Pettigrew, N. R., Churchill, J. H., & Incze, L. S. (2009). Drifter observations of the Gulf of Maine Coastal Current. *Continental Shelf Research*, 29(7), 835–845. <https://doi.org/10.1016/j.csr.2008.12.008>
- Morrison, J. R., Pettigrew, N. R., O'Donnell, J., & Runge, J. A. (2012). *Rapid detection of climate scale environmental variability in the Gulf of Maine*. In 2012 Oceans (pp. 1–5). IEEE.
- Niiler, P. P., Sybrandt, A. S., Kenong, B., Poulain, P. M., & Bitterman, D. (1995). Measurements of the water-following capability of holey-sock and tristar drifters. *Deep-Sea Research I*, 42(11–12), 1961–1964. [https://doi.org/10.1016/0967-0637\(95\)00076-3](https://doi.org/10.1016/0967-0637(95)00076-3)
- Pershing, A. J., Alexander, M. A., Brady, D. C., Brickman, D., Curchitser, E. N., Diamond, A. W., et al. (2021). Climate impacts on the Gulf of Maine Ecosystem: A review of observed and expected changes in 2050 from rising temperatures. *Elementa Science of the Anthropocene*, 9(1), 00076. <https://doi.org/10.1525/elementa.2020.00076>
- Pershing, A. J., Alexander, M. A., Hernandez, C. M., Kerr, L. A., Le Bris, A., Mills, K. E., et al. (2015). Slow adaptation in the face of rapid warming leads to collapse of the Gulf of Maine cod fishery. *Science*, 350(6262), 809–812. <https://doi.org/10.1126/science.aac9819>
- Pettigrew, N. R., Churchill, J. H., Janzen, C. D., Mangum, L. J., Signell, R. P., Thomas, A. C., et al. (2005). The kinematics and hydrographic structure of the Gulf of Maine Coastal Current. *Deep Sea Research II*, 52(19–21), 369–2391.
- Scully, M. E., Geyer, W. R., Borkman, D., Pugh, T. L., Costa, A., & Nichols, O. C. (2022). Unprecedented summer hypoxia in southern Cape Cod Bay: An ecological response to regional climate change? *Biogeosciences*, 19(19), 3523–3536. <https://doi.org/10.5194/bg-19-3523-2022>
- Shchepetkin, A. F., & McWilliams, J. C. (2003). A method for computing horizontal pressure gradient force in an oceanic model with a nonaligned vertical coordinate. *Journal of Geophysical Research*, 108(C3), 3090. <https://doi.org/10.1029/2001JC001047>
- Shchepetkin, A. F., & McWilliams, J. C. (2005). The Regional Oceanic Modeling System (ROMS): A split-explicit, free-surface, topography-following-coordinate oceanic model. *Ocean Modelling*, 9(4), 347–404. <https://doi.org/10.1016/j.ocemod.2004.08.002>
- Sherman, K., & Skjoldal, H. R. (2002). *Large marine ecosystems of the North Atlantic: Changing states and sustainability*. Elsevier.
- Thompson, C. (2010). *The Gulf of Maine in context: State of the Gulf of Maine Report*. Gulf of Maine Counsel on the Marine Environment. Retrieved from <https://www.gulfofmaine.org/state-of-the-gulf/docs/the-gulf-of-maine-in-context.pdf>
- Valigra, L. (2006). Surprising species diversity revealed: Census shows ‘huge reservoir of information about life’ in the Gulf of Maine. *Gulf of Maine Times*, 10(1).
- Wang, Z., Brickman, D., & Greenan, B. J. (2019). Characteristic evolution of the Atlantic Meridional Over-turning Circulation from 1990 to 2015: An eddy-resolving ocean model study. *Deep-Sea Research I*, 149, 103056. <https://doi.org/10.1016/j.dsr.2019.06.002>
- Xue, H., Chai, F., & Pettigrew, N. (2000). A model study of the seasonal circulation in the Gulf of Maine. *Journal of Physical Oceanography*, 30(5), 1111–1135. [https://doi.org/10.1175/1520-0485\(2000\)030<1111:amsots>2.0.co;2](https://doi.org/10.1175/1520-0485(2000)030<1111:amsots>2.0.co;2)
- Xue, H., Incze, L., Xu, D., Wolff, N., & Pettigrew, N. (2008). Connectivity of lobster populations in the coastal Gulf of Maine. Part 1: Circulation and Larval Transport Potential. *Ecological Modelling*, 110(1–2), 193–211. <https://doi.org/10.1016/j.ecolmodel.2007.07.024>
- Zeng, Z., Ziegler, A. D., Searchinger, T., Yang, L., Chen, A., Ju, K., et al. (2019). A reversal in global terrestrial stilling and its implications for wind energy production. *Nature Climate Change*, 9(12), 979–985. <https://doi.org/10.1038/s41558-019-0622-6>